Int. J. Electrochem. Sci., 16 **(2021)** Article ID: 210520, doi; 10.20964/2021.05.16

International Journal of ELECTROCHEMICAL SCIENCE
www.electrochemsci.org

Short Communication

Photocatalytic and electrochemical characteristics of $BiFeO_3$-TiO_2 nanoheterostructure for leather dyes degradation

Qiyan Wang[1], Baorong Duan[1,], Yuzhen Zhao[2], Han Yu[1], Yonggen Weng[1], Tiantian Zhang[1]*

[1] Research Center for Leather and Protein of College of Chemistry & Chemical Engineering, Yantai University, Shandong Yantai, 264005, China
[2] Key Laboratory of Organic Polymer Photoelectric Materials, School of Sciences, Xijing University, Xi'an, 710123, China
[*]E-mail:duanbaorong@126.com

Received: 5 December 2020 / *Accepted:* 16 February 2021 / *Published:* 31 March 2021

The present work was focused on hydrothermal synthesis of the titanium oxide (TiO_2) nanorods and bismuth ferrite ($BiFeO_3$)-TiO_2 nanoheterostructure on indium tin oxide (ITO) as photocatalysts for photodegradation of leather dyes under visible-light irradiation. The samples were characterized via the SEM, XRD, EIS and UV-Vis absorption spectra. SEM results revealed that high density and high aspect ratio of $BiFeO_3$-TiO_2were successfully grown on ITO substrate. XRD analysis exhibits that both the TiO_2 and BiFeO3 phases coexist, which shows that there aren't any impurity phases at the interface between $BiFeO_3$ and TiO_2 with the synthesis condition. Optical characterization results revealed that BiFeO3 nanoparticles leads to reduction the band-gap of TiO_2 nanorods which were calculated to be 2.93 and 2.58 eV for the TiO2 and $BiFeO_3$/TiO_2nanoheterostructure, respectively. EIS analysis shows that $BiFeO_3$/TiO_2 revealed lower recombination rate of electron-hole pairs which accelerate the photocatalytic reactions. The degradation efficiency for $BiFeO_3$/TiO_2 nanoheterostructure was 88% after 90 min under visible-light radiation which was significantly greater than its degradation efficiency (54%) in TiO_2 nanorods. These findings exhibited that the $BiFeO_3$/TiO_2 has the excellent visible-light harvesting performance for degradation of leather dyes.

Keywords: $BiFeO_3$/TiO_2nanoheterostructure; Photocatalysts; Photodegradation of leather dyes; Optical and electrochemical properties

1. INTRODUCTION

Textile and leather dye effluents are one of the major concerns of contamination with azo dyes up to 50% [1, 2]. However, textile dyes have been widely tested for decolonization, studies on leather dyes are still growing [3]. While both leather and textile industries use various common dyes, the effluents produced by both vary in numerous aspects such as concentration, temperature, pH, etc[4, 5].

These pollutants are degraded by advanced oxidative procedures that create hydroxyl radicals as the major oxidant [6, 7]. Hydroxyl radicals are highly efficient oxidizers. Thus, photo-electrocatalytic degradation has been broadly used as an alternative electrochemical method for environmental remediation [8, 9]. Using semiconductor photo-catalysts and UV light can mineralize and degrade these dyes [10].

Titanium oxide (TiO_2)-based photo-catalysts have been used widely for degradation of the organic pollutants to remediate contaminated groundwater, hazardous wastes and controlling the toxic air contaminants [11, 12]. Though, the optical band-gap of TiO2 is wide-ranging that can only absorb UV-light, which is only 5% at the source of sun [13]. Therefore, other classes of oxides for example ferrites with narrowing optical band-gap in the visible-light region have been a great deal of interest in it as a potentially visible catalyst for industrial processes [14-16].

Multiferroic oxides have great potential for multi-functional capabilities in spintronic, random access memory, data storage, attenuators, filters, photovoltaic and sensor devices due to their basic physical properties [17]. Among the multiferroic oxides, $BiFeO_3$ (bismuth ferrite) has received ever-increasing attraction due to its coupling of magnetism and ferroelectricity, promising for fabrication of magnetoelectric devices [18, 19].

This work focused on an efficient approach to attain multi-functionality in $BiFeO_3$ nanomaterial synthesized on wide band-gap TiO_2nanorods substrate. To our best knowledge, the photo-catalysis activities based on the $BiFeO_3$-TiO_2nano-heterostructure have not been considered until now. Here, one-dimensional $BiFeO_3/TiO_2$ nanostructure photocatalysts were synthesized by combining hydrothermal and spin coating techniques. The enhanced photocatalytic activity of $BiFeO_3/TiO_2$ nano-heterostructure can be attributed to the light-harvesting property of $BiFeO_3$ and outstanding charge separation features of the shaped heterojunction between TiO_2 and $BiFeO_3$.

2. MATERIALS AND METHOD

The TiO_2 nanostructures were grown on indium tin oxide (ITO) glass by a hydrothermal technique. The ITO substrate was cut in squares (10×10 mm^2) and cleaned with DI water and acetone. A mixed solution of DI water and hydrochloric acid, with a (1:1) volume ratio, including a suitable volume of $Ti(OC_4H_9)_4$ was utilized for hydrothermal reactions. After that, the ITO was placed in an autoclave including the prepared solution and retained into an oven at 170 °C for 5h. Then, the TiO_2nanorods were synthesized on the ITO substrate. Precursor solution of $BiFeO_3/TiO_2$ was produced by a typical sol-gel method, in which $Fe(NO_3)_3\cdot9H_2O$ and $Bi(NO_3)_3\cdot5H_2O$ were utilized as a starting material. An equimolar volumes of $Bi(NO_3)_3\cdot5H_2O$ and $Fe(NO_3)_3\cdot9H_2O$ and was dissolved into 2-methoxyethanol for obtaining a clear and brown solution via a magnetic stirrer. After that, citric acid as an acidifier and a chelating agent was added in the solution. After one day, the precursor solution ($0.3mol*l^{-1}$) was used for doing experiments. Then, the prepared solution was spin-coated on TiO_2nanorods four times to create uniform wet film. After per step, wet film was primarily dried at 170°C for 10 min for evaporation of all solvent. Then, the film quickly heated to 350°C for 15min to

eliminate the residual organic material. Then, the film was annealed at 500°C for 20min to allow the $BiFeO_3$ for crystallization, and resulting $BiFeO_3/TiO_2$nanoheterostructure were obtained.

The morphology of prepared specimens was considered through scanning electron microscopy (SEM). The X-ray diffractometer with Cu Kα radiation at wavelength of 1.5404Å operating at 30 kV and 20 mA was used to investigate the crystal structures of specimens. EIS tests were done in frequency range from 0.1kHz to 1MHz at 5 mV AC voltage using CHI 660D potentiostat (Chenhua Co. Shanghai, China) in a conventional three-electrode electrochemical cell which includes prepared films, Pt wire and Ag/AgCl electrode as working, counter and reference electrodes, respectively. The electrolyte solution was in 0.1M KCl (99%). Photo-catalysis tests were performed by a photoreaction tool (125 Watt Mercury Lamp) as a light source. Leather dyes were supplied by Luthai Textile Co. Ltd., Shandong, China and was utilized as a model pollutant. The concentration of Leather dyes is25 mg/L. The UV/Vis spectrophotometer (UV-2100, China) was used to measure the absorbance spectra of the Leather dye.

3. RESULTS AND DISCUSSION

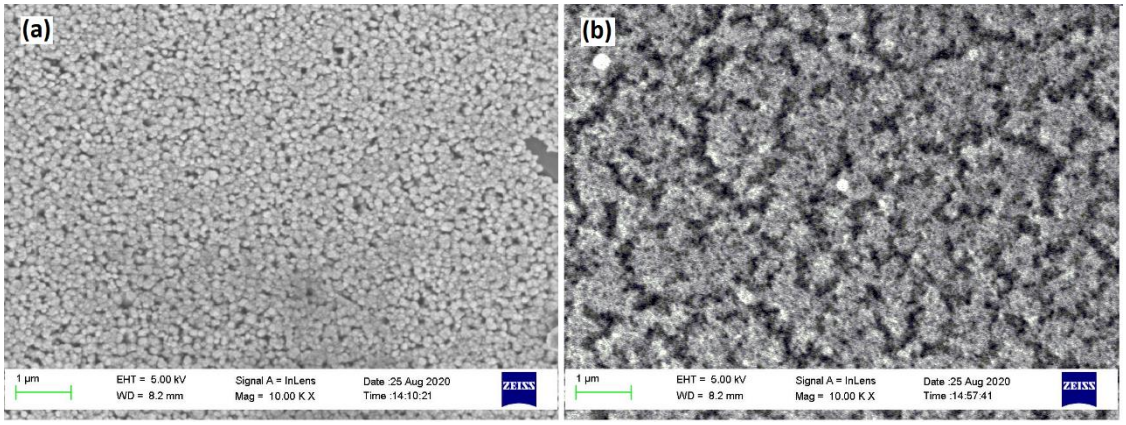

Figure 1. FESEM images of the (a) TiO_2 nanorods and (b) $BiFeO_3/TiO_2$ nano-heterostructure

Figure 1 shows the FESEM images of the TiO_2 nanorods and $BiFeO_3/TiO_2$ nano-heterostructure. As shown in Fig. 1a, the nanorods were synthesized on the surface of ITO and were along the vertical direction to the ITO substrate. The TiO_2 nanostructures had rough square top and smooth side facets. Figure 1b indicates that after spin-coating $BiFeO_3$ onto the TiO_2 nanorods, the TiO_2 nanostructures may not be detected from the FESEM images, but the $BiFeO_3$ crystalline particles can be found.

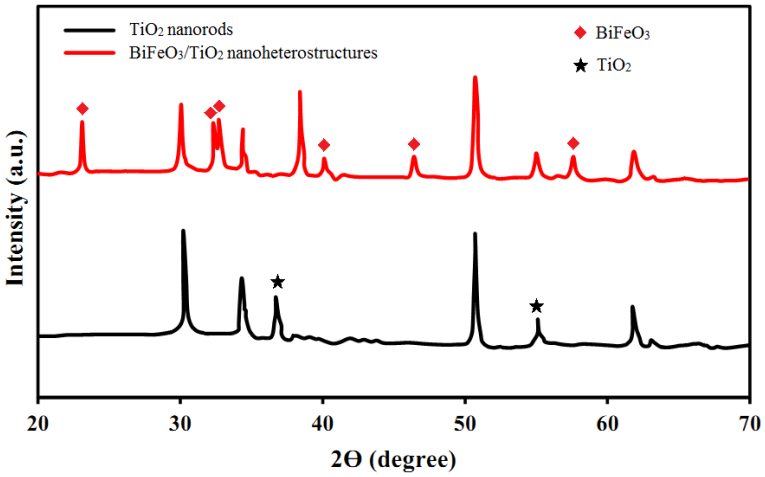

Figure 2. XRD patterns of the TiO_2 nanorods and BiFeO3/TiO2 nano-heterostructurewith Cu Kα radiation at wavelength of 1.5404Å operating at 30 kV and 20 mA

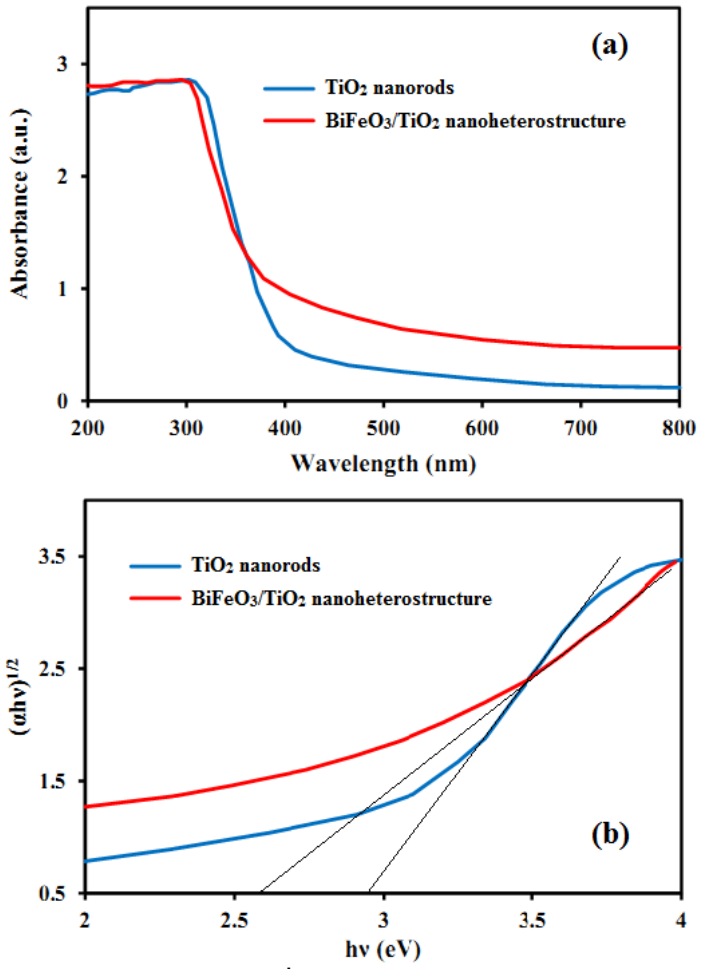

Figure 3. (a) UV-visible absorption spectra and (b) the band gap calculation through Tauc method for the TiO_2nanorods and $BiFeO_3/TiO_2$ nano-heterostructure on ITO

Figure 2 reveals the XRD patterns of the TiO_2nanorods and $BiFeO_3/TiO_2$ nano-heterostructure on ITO. All diffraction peaks are indicated in Fig. 2 except ITO. For TiO_2nanorods synthesized on ITO, the chief diffraction peaks appeared at about 36.7° and~55.3°, which associated with (101) and (211) crystal planes of TiO_2 structures (JCPDS Card No.21-1272) [20]. The diffraction peaks of perovskite phase $BiFeO_3$ are labeled with red color (JCPDS card No.86-1518), which indicates that well-crystallized $BiFeO_3$ may be attained by the synthesis condition. Furthermore, the XRD pattern of $BiFeO_3/TiO_2$nanoheterostructure exhibit that both TiO_2 and BiFeO3 phases coexist, which shows that there aren't any impurity phases at interface between $BiFeO_3$ and TiO_2 with synthesis condition.

The UV-visible absorption spectra of the samples are shown in Figure 3. The absorption spectra indicate that the $BiFeO_3$ nanostructures can absorb significant amounts of visible light, signifying their potential application as visible-light photo-catalysts. It can be attributed to the small intrinsic band-gap of $BiFeO_3$. The optical direct band-gap (Eg) may be calculated by the following equation [21]:

$$(\alpha h\nu)^2=A(h\nu-Eg) \quad (1)$$

where hν shows the photon energy, α and A are the absorption coefficient and a material dependent constant, respectively [22]. The measured band-gap of the TiO2 and $BiFeO_3/TiO_2$ nano-heterostructure were calculated to be 2.93 and 2.58 eV, respectively. The band-gap energy decreased with spin coating of the $BiFeO_3$ on TiO_2 nanorods because of the quantum-size effect.

Moreover, electrons and holes can be created in the semiconductor band structure under UV-Vis light irradiation. The photo-generated charge-carrier may enhance the photocatalytic activities [23]. As a result, spin coating of $BiFeO_3$ can prevent the recombination of holes and electrons, improving the catalytic activities and make robust light-harvesting abilities.

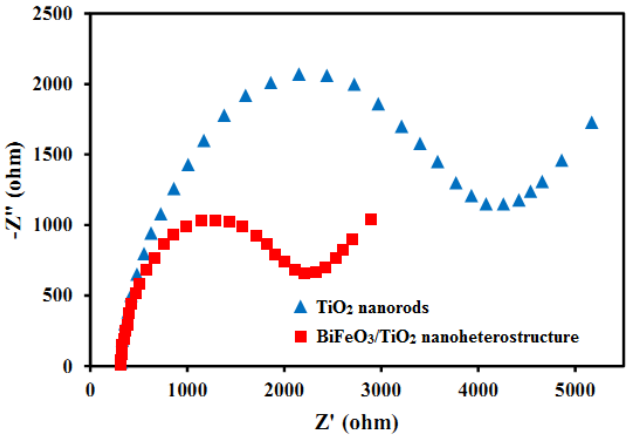

Figure 4. Nyquist plots of TiO2 nanorods and BiFeO3/TiO2 nano-heterostructure visible-light irradiation with frequency range of 0.1kHz to 1MHz at 5 mV applied voltage into 0.1M KCl (99%)

To further explore the charge-transfer behaviors EIS assessment is a powerful method to analyze the charge-transfer mechanisms at the solution/photocatalyst interface [24]. In the Nyquist plots, the EIS semicircle diameter indicates charge-transfer resistance (R_{ct}) of sample surface. For photocatalytic reaction, a reduction in the R_{ct} value always means a faster charge-transfer and slower

recombination of holes and photoelectrons occurred, which is helpful for relevant photocatalytic activity. As shown in Figure 4, the semicircle radius reduces in the $BiFeO_3/TiO_2$nanoheterostructure sample. An R_{ct} of 4840 Ω was obtained for TiO_2nanorods, which was much bigger than the other specimen, proposing that the TiO_2nanorods under visible-light irradiation require overcoming a great energy-barrier to occur in a photocatalytic reaction. In $BiFeO_3/TiO_2$ sample, The R_{ct} was sharply decreased to 2620 Ω, indicating that the close contact of TiO_2 with $BiFeO_3$ was rather efficient in elimination of the hole-electron recombination and acceleration of the photocatalytic reaction. As a result, more long-lived photo-generated electrons contribute with the photo-degradation organic pollutants [25].

In order to study the photocatalytic degradation behavior of the prepared $BiFeO_3/TiO_2$ nano-heterostructure in visible-light radiation, the direct irradiation (Blank), TiO_2 nanorods and $BiFeO_3/TiO_2$nanoheterostructurewere used to test. As shown in Figure 5a that the leather dye content of the blank has practically no variation under visible-light, which indicates that leather dyes are difficult to degradation by visible-light alone. In TiO_2 nanorods and $BiFeO_3/TiO_2$ nano-heterostructure, leather dye degradation was clearer, which confirmed that leather dye was removed via catalyst under visible radiation.

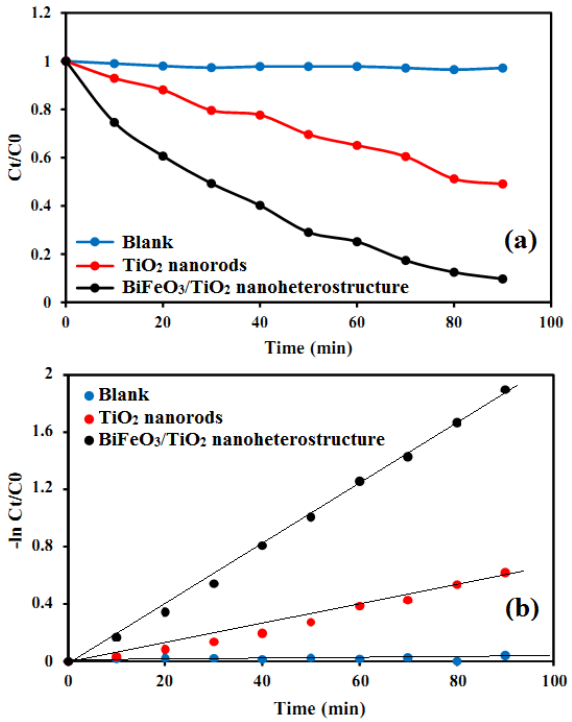

Figure 5. (a) Photodegradation leather dye performance and (b) degradation ratefor 25 mg/L Leather dyes in visible-light radiation.

Clearly, the degradation efficiency of $BiFeO_3/TiO_2$ was considerably higher than degradation efficiency of TiO_2 nanorods. After 90 min of visible irradiation, the removal efficiency of leather dye

reached 88%. The synthesized $BiFeO_3/TiO_2$ was an outstanding photocatalyst and had a good application in organic removal and degradation. As shown in Figure 5b, the $-\ln C_t/C_0$ consistent with each photocatalyst was fundamentally linearly associated with reaction time t, therefore revealing that leather dye degradation followed pseudo-first order kinetics. Reaction rate constant (k) for blank, TiO_2nanorods and $BiFeO_3/TiO_2$ nano-heterostructure are 0.00046, 0.0068 and 0.021 min^{-1}, respectively.$BiFeO_3/TiO_2$ had the robust visible-light photocatalytic activity. Compared with TiO_2, the photocatalytic degradation behavior was significantly enhanced by the $BiFeO_3$. $BiFeO_3$ nanoparticles improved the visible-light absorption of $BiFeO_3/TiO_2$, and improved its visible-light utilization. The prepared $BiFeO_3/TiO_2$nanoheterostructure had regular and uniform morphologies, and more active sites for dye adsorption were exposed on the surface of crystal, which was favorable for the utilization of visible-light and the adsorption of leather dye [26]. The presence of $BiFeO_3$ nanoparticles leads to the creation of photoexcited electron-hole pairs in TiO_2 nanorods under visible-light irradiation [27]. It can promote the separation of holes and electrons and delay their recombination. It significantly enhances the photocatalytic performance. Furthermore, $BiFeO_3/TiO_2$ could better prepare more catalytic current than bare TiO_2 under visible-light. Hence, it seriously increased the free carrier content, activated radicals and facilitated the creation of stronger oxidizing holes (h^+) and then accelerated leather dye removal and degradation.

Comparison the photodegradation efficiency of leather dye on $BiFeO_3/TiO_2$ nano-heterostructure with other nanostructured photocatalysts is presented in Table 1. As seen, by considering the time of photodegradation, $BiFeO_3/TiO_2$ nano-heterostructure show the degradation efficiency of 88% for 90 min, which are higher than the reported degradation efficiency values in [28-31].

Table 1. Comparison of degradation efficiency of leather dye on $BiFeO_3/TiO_2$ nano-heterostructurewith other nanostructured photocatalysts

Photocatalysts	**Leather dye concentration (mg l^{-1})**	**Time (minutes)**	**Degradation efficiency (%)**	**Ref.**
La doped Nb_2O_5	100	100	80	[28]
CeO2–SnO2 Nanocomposite	50	240	50	[29]
Laccase	20	360	75	[30]
CS-ZnS-NPs	30	165	92	[31]
$BiFeO_3/TiO_2$	25	90	88	This work

4. CONCLUSIONS

Textile and leather dye effluents are one of the major concerns of contamination with azo dyes. This work was focused on hydrothermal synthesis of the TiO_2 nanorods and $BiFeO_3$-TiO_2 nano-

heterostructure on ITO glass substrate as photocatalysts for photodegradation of leather dyes under visible-light irradiation. The samples were characterized via the SEM, XRD, EIS and UV-Vis absorption spectra. SEM results revealed that high density and high aspect ratio of $BiFeO_3$-TiO_2 were successfully grown on ITO substrate. XRD analysis exhibits that both TiO_2 and BiFeO3 phases coexist, which shows that there aren't any impurity phases at the interface between $BiFeO_3$ and TiO_2 with the synthesis condition. Optical characterization results revealed that $BiFeO_3$ nanoparticles improved the visible-light absorption of $BiFeO_3/TiO_2$, and improved its visible-light utilization. EIS analysis shows that $BiFeO_3/TiO_2$ revealed lower recombination rate of electron-hole pairs which accelerate the photocatalytic reactions. The degradation efficiency for $BiFeO_3/TiO_2$ nano-heterostructure was 88% after 90 min under visible-light radiation which was significantly greater than its degradation efficiency (54%) in TiO_2 nanorods. These results exhibited that the $BiFeO_3/TiO_2$ increased the free carrier content, activated radicals and facilitated the creation of stronger oxidizing holes (h^+) and then accelerated leather dye removal and degradation.

References

1. P.A. Carneiro, G.A. Umbuzeiro, D.P. Oliveira and M.V.B. Zanoni, *Journal of hazardous materials*, 174(2010)694.
2. H. Karimi-Maleh, M. Alizadeh, Y. Orooji, F. Karimi, M. Baghayeri, J. Rouhi, S. Tajik, H. Beitollahi, S. Agarwal and V.K. Gupta, *Industrial & Engineering Chemistry Research*, 60(2021)816.
3. B.L. Alderete, J. da Silva, R. Godoi, F.R. da Silva, S.R. Taffarel, L.P. da Silva, A.L.H. Garcia, H.M. Júnior, H.L.N. de Amorim and J.N. Picada, *Chemosphere*, 263(2020)128291.
4. V. Selvaraj, T.S. Karthika, C. Mansiya and M. Alagar, *Journal of molecular structure*, 12(2020)129195.
5. J. Rouhi, S. Kakooei, S.M. Sadeghzadeh, O. Rouhi and R. Karimzadeh, *Journal of Solid State Electrochemistry*, 24(2020)1599.
6. Q. Mei, J. Sun, D. Han, B. Wei, Z. An, X. Wang, J. Xie, J. Zhan and M. He, *Chemical Engineering Journal*, 373(2019)668.
7. R. Mohamed, J. Rouhi, M.F. Malek and A.S. Ismail, *International Journal of Electrochemical Science*, 11(2016)2197.
8. R. Montenegro-Ayo, J.C. Morales-Gomero, H. Alarcon, A. Corzo, P. Westerhoff and S. Garcia-Segura, *Chemosphere*, 18(2020)129320.
9. H. Karimi-Maleh, S. Ranjbari, B. Tanhaei, A. Ayati, Y. Orooji, M. Alizadeh, F. Karimi, S. Salmanpour, J. Rouhi and M. Sillanpää, *Environmental Research*, 195(2021)110809.
10. Z.S. Seddigi, M.A. Gondal, U. Baig, S.A. Ahmed, M. Abdulaziz, E.Y. Danish, M.M. Khaled and A. Lais, *PloS one*, 12(2017)e0172218.
11. C.C. de Escobar, Y.P.M. Ruiz, J.H.Z. dos Santos and L. Ye, *Colloids and Surfaces A: Physicochemical and Engineering Aspects*, 538(2018)729.
12. S. Kang, L. Zhang, C. Liu, L. Huang, H. Shi and L. Cui, *International Journal of Electrochemical Science*, 12(2017)5284.
13. Y. Li, K. Lv, W. Ho, F. Dong, X. Wu and Y. Xia, *Applied Catalysis B: Environmental*, 202(2017)611.
14. R.B. Marcelino and C.C. Amorim, *Environmental Science and Pollution Research*, 26(2019)4155.

15. M. Aiempanakit, T. Tabtimsri, N. Triamnak and C. Suwanchawalit, *International Journal of Electrochemical Science*, 14(2019)1954.
16. H. Karimi-Maleh, Y. Orooji, A. Ayati, S. Qanbari, B. Tanhaei, F. Karimi, M. Alizadeh, J. Rouhi, L. Fu and M. Sillanpää, *Journal of Molecular Liquids*, (2020)115062.
17. B. Zhang, J. Huang, B.X. Rutherford, P. Lu, S. Misra, M. Kalaswad, Z. He, X. Gao, X. Sun and L. Li, *Materials Today Nano*, 26(2020)100083.
18. A. Malathi, P. Arunachalam, V. Kirankumar, J. Madhavan and A.M. Al-Mayouf, *Optical Materials*, 84(2018)227.
19. J. Rouhi, S. Kakooei, M.C. Ismail, R. Karimzadeh and M.R. Mahmood, *International Journal of Electrochemical Science*, 12(2017)9933.
20. H. Xiong, L. Wu, Y. Liu, T. Gao, K. Li, Y. Long, R. Zhang, L. Zhang, Z.A. Qiao and Q. Huo, *Advanced Energy Materials*, 9(2019)1901634.
21. M. Isik, S. Delice, H. Nasser, N. Gasanly, N. Darvishov and V. Bagiev, *Materials Science in Semiconductor Processing*, 120(2020)105286.
22. K. Aly, Y. Saddeek and A. Dahshan, *Optical Materials*, 109(2020)110341.
23. G.D. Gesesse, C. Li, E. Paineau, Y. Habibi, H. Remita, C. Colbeau-Justin and M.N. Ghazzal, *Chemistry of Materials*, 31(2019)4851.
24. M. Ji, J. Xia, J. Di, Y. Liu, R. Chen, Z. Chen, S. Yin and H. Li, *Chemical Engineering Journal*, 331(2018)355.
25. X. Dai, Z. Jiao, Z. Ma, K. Liu, C. Wang and H. Su, *The Journal of Physical Chemistry C*, 123(2019)20325.
26. S. Iqbal, A. Bahadur, S. Anwer, S. Ali, R.M. Irfan, H. Li, M. Shoaib, M. Raheel, T.A. Anjum and M. Zulqarnain, *Colloids and Surfaces A: Physicochemical and Engineering Aspects*, 601(2020)124984.
27. L. Di, H. Yang, T. Xian and X. Chen, *Materials*, 10(2017)1118.
28. G. Collazzo, D. Paz, S. Jahn, N. Carreño and E. Folleto, *Latin American applied research*, 42(2012)51.
29. E.L. Foletto, S. Battiston, G.C. Collazzo, M.M. Bassaco and M.A. Mazutti, *Water, Air, & Soil Pollution*, 223(2012)5773.
30. A. Pandi, G.M. Kuppuswami, K.N. Ramudu and S. Palanivel, *Journal of Cleaner Production*, 211(2019)590.
31. A. Aziz, N. Ali, A. Khan, M. Bilal, S. Malik, N. Ali and H. Khan, *International journal of biological macromolecules*, 153(2020)502.